

"This document is intended for publication in the open literature. It is made available on the understanding that it may not be further circulated and extracts may not be published prior to publication of the original, without the consent of the Publications Officer, JET Joint Undertaking, Abingdon, Oxon, OX14 3EA, UK".

"Enquiries about Copyright and reproduction should be addressed to the Publications Officer, JET Joint Undertaking, Abingdon, Oxon, OX14 3EA".

ANALYSIS OF EMISSION SPECTRA FROM MARFES IN JET

M G O'Mullane¹, I H Coffey², N J Peacock³, R Giannella, R Reichle

JET Joint Undertaking, Abingdon, Oxon., OX14 3EA, UK

¹*University College Cork, Ireland,* ²*Queens University Belfast, Northern Ireland,*

³*UKAEA (Government Division) Fusion, Culham Laboratory, Abingdon Oxon., UK*

Abstract

The emission spectra from MARFES (Multifaceted Asymmetric Radiation From the Edge) is examined. These condensation phenomena occur in tokamak plasmas and are toroidally symmetric but have poloidal asymmetry. Emission spectra, from XUV and VUV instruments on JET (Joint European Torus), are analysed to deduce the parameters of a typical MARFE. All atomic data and modelling codes form part of the ADAS system [1] at JET.

1. Introduction

Condensation phenomena are well-known in astrophysical plasmas; e.g. solar prominences [2]. In tokamak plasmas a radiative condensation can result in a localised region of edge plasma becoming cooler and denser than the surrounding background plasma yet remaining in pressure balance [3]. A trigger event, such as a local influx of neutral fuel ions or an MHD instability can cause this local cooling. One of the unusual properties of MARFES is that while they are toroidally symmetric they do not follow the magnetic field lines and are poloidally asymmetric. The toroidal symmetry is an assumption of most models and wide angle views of the plasma tend to confirm this hypothesis.

MARFES are usually located near the inner wall on the high field side of the torus. Their position is determined by the ion ∇B drift. The MARFE region can remain stationary for 1 – 2s or can oscillate poloidally at frequencies of 20Hz. Figure 1 shows the location of a typical MARFE with the viewing lines of the XUV and VUV spectrometers available at JET. The size has been inferred from a multi-cord bolometer which views the inner wall.

A related phenomenon is the X-point (or 'divertor') MARFE. During radiative divertor experiments nitrogen (or neon) is puffed into the divertor to cause the plasma to detach from the target plates. Large amounts of power (up to 80% of input power) are radiated in $\sim 10\%$ equivalent plasma volume. There are large temperature and density gradients

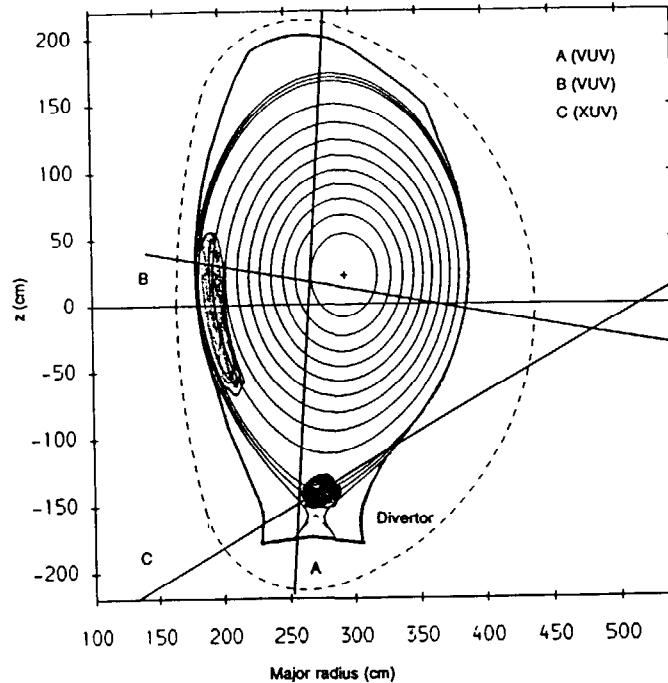


Fig. 1. Poloidal cross-section of JET with magnetic flux surfaces. Also shown are the lines-of-sight of the XUV (Schwob) and VUV (SPRED) spectrometers in JET. The locations of the inner wall MARFE and divertor MARFE are shaded.

parallel to the magnetic field which are ideal conditions for MARFE formation. Following detachment a region of strong emission is observed near the X-point inside the separatrix. The emission region remains stable for 1 – 2s. This is the ‘divertor’ MARFE.

2. Model of Impurities in a MARFE

The MARFE is sustained by the balance between parallel heat conduction from the surrounding plasma and local radiation losses. When the radiation exceeds the heat inflow and $\partial P_{\text{rad}}/\partial T_e$ of impurity radiation is at a minimum the MARFE forms. Low temperatures near the plasma edge and the shape of the impurity radiation curves (P_{rad}) ensure that low Z elements are the causal impurities in MARFE formation at temperatures of $\sim 15\text{eV}$.

Two sources of impurities can give rise to MARFE radiation *viz.* existing bulk impurities streaming through the MARFE along the field lines and influxes of fresh impurities from the vessel wall. The initial distribution of ionisation stages reflects the origin of the sources (i.e. neutral or reflecting the local diffusive ionisation balance of $T_e \geq 100\text{eV}$). The MARFE alters the edge conditions but the radial distribution of impurity ionisation stages is not significantly affected since the re-ionisation time of a particle leaving the MARFE is shorter than its transit time around the torus. The time taken for incoming ions to attain MARFE temperatures, the thermalisation time, is $\sim 10^{-7}\text{s}$, faster than atomic processes. The subsequent evolution of the impurities in the MARFE is determined by their residence time and the atomic timescales. Populations of ionisation stages

out of coronal equilibrium are given by the set of coupled equations ($i = 1, Z$)

$$\frac{\partial n_z}{\partial t} + \nabla \cdot \Gamma_z = n_e [-n_z S_z + n_{z-1} S_{z-1} - n_z \alpha_z + n_{z+1} \alpha_{z+1}] \quad (1)$$

where S_z and α_z are ionisation and recombination coefficients.

The passage of impurities through the MARFE depends on the collisional regime they encounter. The frictional slowing down time (τ_{\parallel}) determines their motion along the field lines and modifies their parallel velocities from $\frac{1}{3}v_{\text{thermal}}$. The diffusive deflection time (τ_{\perp}) governs the motion perpendicular to the flux surfaces. Over a range of MARFE temperatures and densities these times are comparable and of the order of a few milliseconds. This is also the timescale to establish ionisation equilibrium in the MARFE. The residence time is estimated at ~ 10 ms. The solution of (1) is simplified by replacing the transport term ($\nabla \cdot \Gamma_z$) by (n_z/τ_p) with a confinement time (τ_p) common to all ionisation stages.

The emission in a particular spectrum line is composed of separate independent parts driven by excitation, recombination and possibly charge exchange. The emission from these processes is calculated using ADAS. The total line emission is constructed from these and the time varying ionisation balance.

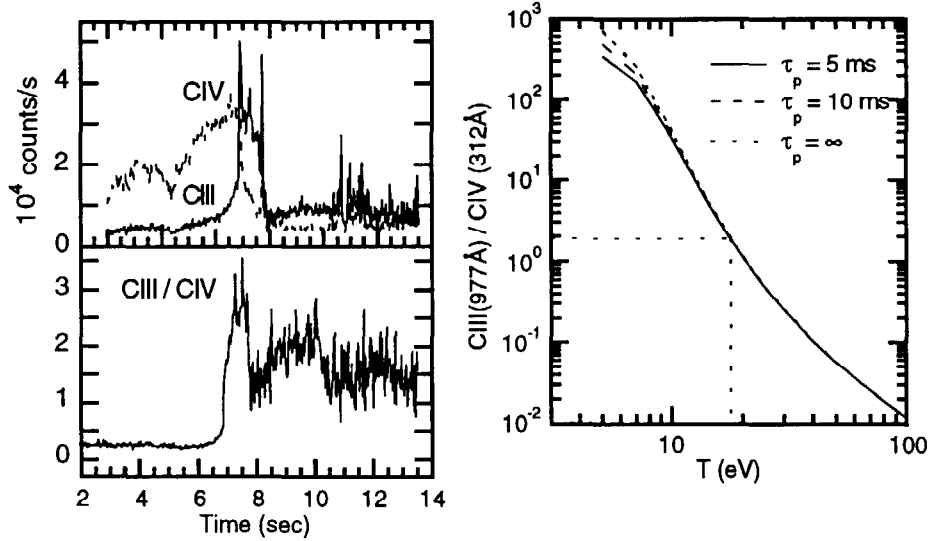


Fig. 2. Variation of CIII, CIV and their ratio (left) during an inner wall MARFE from spectrometer B. The MARFE appears at 6.7s. The calculated ratio is also shown (right) for a 10ms residence time. The dotted line indicates a ratio of 2.0

3. Plasma Parameters of Inner Wall MARFE

Inner wall MARFES form during the limiter phase of the discharge when there is no stabilising divertor. They are characterised by a sharp rise in radiation which usually exceeds the input power. Following some trigger (an influx from plasma-wall interaction) the total radiation increases and becomes localised, as a MARFE, on the inner wall. The localised radiation is accompanied by enhanced deuterium Lyman α (D_α) indicating

cooler temperatures. During the MARFE charge exchange features between incoming bare ions and deuterium (e.g. C^{6+} , $n = 4 - 3$ line at 521\AA) have been observed.

The inner wall MARFE occasionally lies along the line-of-sight of spectrometer 'B'. Figure 2 shows that the CIV $1s^2 2s^2 S - 1s^2 3p^2 P$ 312.4\AA line falls with a simultaneous rise in the CIII $2s^2 ^1S_0 - 2s2p ^1P_1$ 977\AA line indicating that this emission comes from recombining carbon. The transient model, described in section 2, is used to interpret this ratio since these lines are from adjacent ionisation stages. Calculations show that this line ratio is sensitive to temperature. This recombining model suggests that the MARFE temperature is $\sim 16 - 18\text{eV}$. Calculated ratios corresponding to the observed value do not vary greatly with integration time indicating that the carbon has attained near ionisation equilibrium values in the MARFE. The sensitivity of this ratio on confinement time (τ_p) and density is most marked at temperatures below 12eV and can be neglected in this analysis.

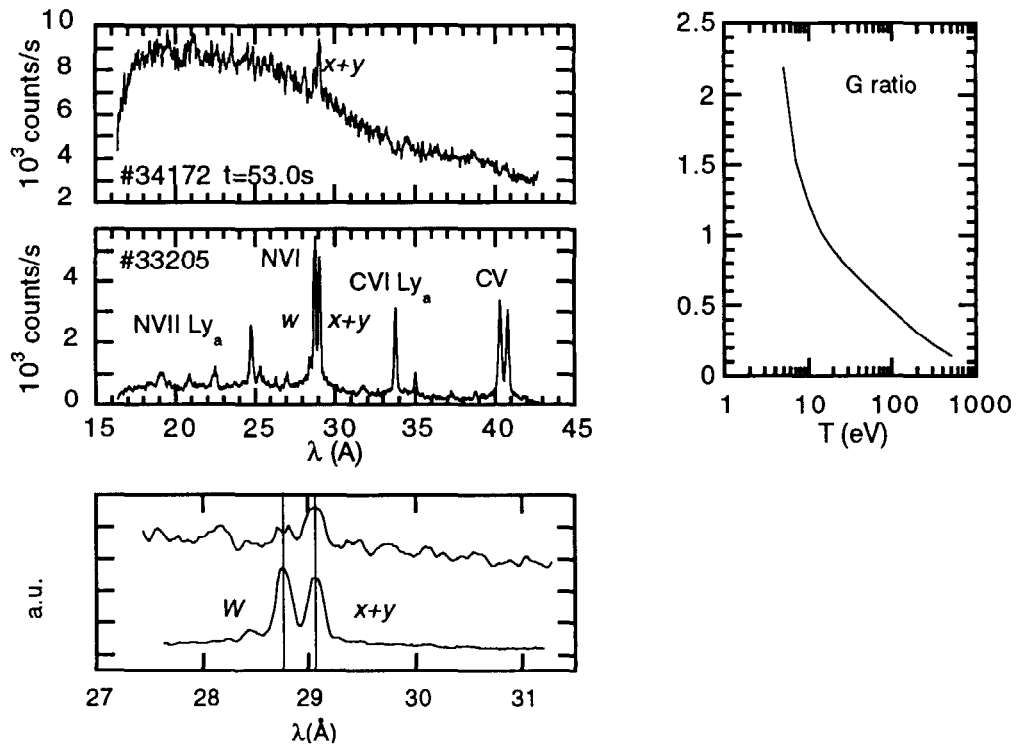


Fig. 3. NVI and NVII in a 'divertor' MARFE discharge (top left) compared to standard nitrogen emission (middle left) in the absence of a MARFE. The NVI shown in greater detail (bottom left). The Nitrogen G ratio in coronal balance is also shown (right).

4. Plasma Parameters of X-point MARFE

The divertor region is monitored by spectrometers 'A' (VUV) and 'C' (XUV) with intersecting lines-of-sight which together give spectral coverage of NII-NVII. When nitrogen is puffed the nitrogen radiation swamps the intrinsic carbon. In the VUV the dominant ionisation stages are NIV and NV with NIII rising throughout the gas puffing phase. The ionisation balance temperatures is $\sim 20\text{eV}$.

The XUV spectrometer shows no evidence of strong radiation from H- and He-like

nitrogen during the radiative divertor phase. The NVI intercombination line becomes the strongest NVI line indicative of a strongly recombining plasma. The expanded NVI spectrum of figure 3 (bottom left) shows the absence of the resonance line. The calculated G ratio (intercombination $(1s^2\ ^1S_0 - 1s2p\ ^3P_1)$ / resonance $(1s^2\ ^1S_0 - 1s2p\ ^1P_1)$; $x + y/w$) in coronal equilibrium indicates that a large G ratio is a measure of low electron temperature. Irrespective of the equilibrium conditions the 'observed' G ratio indicates very cold temperatures of less than 10eV in the X-point MARFE.

5. Discussion and Conclusions

It remains to directly measure the temperature and density of a MARFE simultaneously. MARFES are in pressure balance. Appropriate diagnostics are required to test whether there is a concomitant rise in density. The toroidal symmetry also remains to be confirmed experimentally. Streaming particles through the MARFE will leave a recombination dominated spectrum. A contiguous spectral coverage (5 – 3000Å perhaps?) is necessary to reconcile the fragmentary observations with such theories.

XUV and VUV observations of MARFES have been interpreted and suggest electron temperatures of 16eV for inner wall MARFES with somewhat lower temperatures for the divertor MARFE. Transport within the MARFE is different from that of the surrounding plasma and the collisionality may be high enough to retain impurities for a sufficient time for them to attain ionisation equilibrium.

Acknowledgements

This work has been jointly funded by the UK Department of Trade and Industry and by EURATOM.

1. Summers, H. P., 1994, *The Atomic Data and Analysis Structure (ADAS) User Manual* JET Internal Report, JET-IR(94)06
2. Parker, E. N., 1953, *Astrophys. J.* **117** 431.
3. Lipschultz, B., 1987, *J. Nucl. Mater.* **145–147** 15.